

## OPTICA

## Few-femtosecond soft X-ray transient absorption spectroscopy with tuneable DUV-Vis pump pulses

JACOB P. LEE,<sup>1</sup> TIMUR AVNI,<sup>1</sup> OLIVER ALEXANDER,<sup>1</sup> MARIOS MAIMARIS,<sup>2</sup> HAOQING NING,<sup>2</sup> ARTEM A. BAKULIN,<sup>2</sup> PHILIPPE G. BURDEN,<sup>3</sup> EVANGELOS MOUTOULAS,<sup>4</sup> DIMITRA G. GEORGIADOU,<sup>4</sup> CHRISTIAN BRAHMS,<sup>5</sup> D JOHN C. TRAVERS,<sup>5</sup> D JON P. MARANGOS,<sup>1</sup> AND CLÉMENT FERCHAUD<sup>1,\*</sup> D

- <sup>1</sup>Department of Physics, Blackett Laboratory, Imperial College London, London SW7 2BW, UK
- <sup>2</sup>Department of Chemistry and Centre for Processable Electronics, Imperial College London, London W12 0BZ, UK
- <sup>3</sup>Department of Physics, University of Ottawa, Ottawa, Ontario K1N 6N5, Canada
- <sup>4</sup>Electronics and Computer Science & Optoelectronics Research Centre, University of Southampton, Southampton SO17 1BJ, UK
- <sup>5</sup>School of Engineering and Physical Sciences, Heriot-Watt University, Edinburgh EH14 4AS, UK
- \*c.ferchaud@imperial.ac.uk

Received 23 May 2024; revised 20 August 2024; accepted 31 August 2024; published 16 September 2024

Achieving few-femtosecond resolution for a pump-probe experiment is crucial to measuring the fastest electron dynamics and for creating superpositions of valence states in quantum systems. However, traditional UV-Vis pump pulses cannot achieve few-fs durations and usually operate at fixed wavelengths. Here, we present, to our knowledge, an unprecedented temporal resolution and pump tuneability for UV-Vis-pumped soft X-ray transient absorption spectroscopy. We have combined few-fs deep-UV to visible tuneable pump pulses from resonant dispersive wave emission in hollow capillary fiber with attosecond soft X-ray probe pulses from high harmonic generation. We achieve sub-5-fs time resolution, sub-fs interferometric stability, and continuous tuneability of the pump pulses from 230 to 700 nm. We demonstrate that the pump can initiate an ultrafast photochemical reaction and that the dynamics at different atomic sites can be resolved simultaneously. These capabilities will allow studies of the fastest electronic dynamics in a large range of photochemical, photobiological and photovoltaic reactions.

Published by Optica Publishing Group under the terms of the Creative Commons Attribution 4.0 License. Further distribution of this work must maintain attribution to the author(s) and the published article's title, journal citation, and DOI.

https://doi.org/10.1364/OPTICA.530964

Electronic coherences in photochemical reactions, which may determine reaction outcomes, decay on the timescale of 1–10 fs, and the fastest nuclear motion is on a similar timescale [1]. Timeresolved X-ray absorption spectroscopy (TR-XAS) is a powerful tool for studying some of these fastest processes in nature [2]. It has allowed the probing of nuclear and electronic dynamics of molecules on the femtosecond timescale in multiple phases of matter [3–6]. High harmonic generation (HHG) provides an excellent source of broadband attosecond pulses from the extreme ultraviolet into soft X-rays (SXRs) with pulse durations on the scale of tens

to hundreds of attoseconds [7,8]. To probe photochemical reactions on the ultrafast timescale, the attosecond X-ray probe must be preceded by a pump pulse to initiate the electronic dynamics. This is typically a single photon in the ultraviolet-visible (UV-Vis) range [3] or multiple low-energy photons in multiphoton or strong field ionization pump regimes [9].

Producing intense few-fs UV pulses by frequency upconversion is highly challenging due to the limited phase-matching bandwidth and the low conversion efficiency for short pulses. The wavelength is also set by the fundamental wavelength of the available femtosecond lasers; therefore experiments are limited to photochemical systems that can be pumped by these harmonics. Almost every material and even air begin to be absorbent in this region, and at the same time propagation introduces a lot of dispersion, making the generation, transport, and characterization of ultrashort UV pulses extremely challenging. On the other hand, as almost all molecules resonantly absorb radiation in the UV and/or visible, generating pump pulses in this part of the optical spectrum has huge potential for probing excited state electronic dynamics while not ionizing the molecule or material. Recent studies have demonstrated the generation of tuneable, intense, sub-10-fs pulses in the UV-Vis with broadband sum-frequency generation (SFG) [10], achromatic second harmonic generation [11], or with hollow capillary fibers (HCFs) using non-linear mode mixing [12] or cross-phase modulation [13]. While promising, these methods only provide limited tuneability and/or limited pulse energy.

Infrared strong-field ionization pump pulses are usually shorter than single-photon UV-Vis pumps in TR-XAS setups [14,15]. The strong-field regime, however, induces AC Stark distortions of the atomic spectrum, can lead to additional multiphoton channels, and suffers from being less representative of natural photochemical processes that are more typically induced by a single photon. It should be noted that ionization-initiated electron dynamics on the attosecond timescale have been measured [16], but this required pumping with attosecond X-ray pulses in an X-ray free-electron-laser facility (XFEL). When coupled with optical pumps, XFELs

Fig. 1. Schematic diagram of the experimental setup for TR-XAS. uJ-level few-fs tuneable pump pulses are produced via resonant dispersive wave emission in an HCF with the few-cycle signal. Attosecond soft X-ray probe pulses are produced via high harmonic generation with the few-cycle idler. Diff.: differential, achro. HWP: achromatic half-wave plate, ID: inner diameter.

suffer from synchronization jitter, preventing measurements in neutral matter with few-fs resolution.

It is clear that to improve upon the capabilities of TR-XAS systems, higher-energy, UV-Vis tuneable, few-fs pulses are required. Technology to achieve this was recently realized by the generation of resonant dispersive wave (RDW) emission in gas-filled capillary fibers [17]. The energy scalability of the soliton self-compression and RDW processes have been demonstrated with the help of larger core capillaries. The RDW process in HCF can generate widely tuneable few-fs pulses with an energy exceeding the microjoule level [17,18]. RDW emission is therefore a revolutionary new way to pump photochemical systems that overcome many limitations of traditional pumping regimes.

Here, we present a table-top setup that combines isolated attosecond SXR probe pulses from HHG with few-fs UV-Vis tune-able pump pulses from RDW emission to study a large range of photochemical systems with, to the best of our knowledge, unprecedented tuneability and time resolution for UV-Vis-pumped TR-XAS. We present the system capabilities in detail and its capacity to pump and probe an ultrafast photochemical reaction.

The laser system consists of a 1-kHz Ti:Sapphire chirped pulse amplifier (CPA) (KM Labs & Crunchtec) pumping a high-energy optical parametric amplifier (OPA) (HE-TOPAS). Both the idler and signal are spectrally broadened in HCFs and compressed to reach the few-cycle regime (Fig. 1).

The probe pulses are generated via HHG from the idler pulses. This attosecond probe beamline has been previously presented in detail in [4,19-21]. The passively carrier-envelope phase stable idler pulses (1.75 µm) are broadened in a stretched HCF and then compressed to 10.8 fs (1.8 optical cycle, Fig. 2). The pulses enter a vacuum chamber, traverse a delay line with 300 as delay precision, and are then focused on a needle gas cell backed with 2.5 bar of neon, reaching an intensity of  $\sim 2.5 \text{ PW/cm}^2$  and experiencing strong self-compression [20]. After passing through a 100-nmthick titanium filter, used to remove the infrared driving pulse, the generated HHG beam is reimaged on the sample target with a gold-coated toroidal mirror. The transmitted HHG spectrum is then analyzed with a flat-field X-ray spectrometer. The probe spectrum, extending in the water-window region, covers simultaneously multiple atomic edges [Fig. 2(c)]. We have confirmed, with a carrier-envelope-phase scan, that an isolated pulse is generated through ionization gating [20]. Moreover multiple groups have now reported isolated pulse durations between 43 and 322

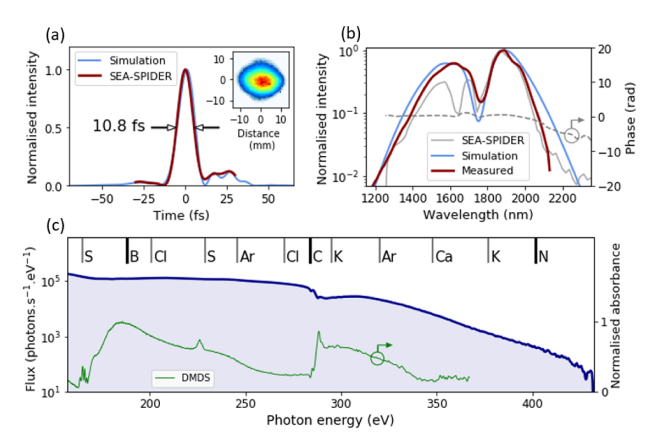


**Fig. 2.** (a) Temporal profile of the few-cycle idler pulses used to drive the HHG process. Inset: idler beam profile. (b) Reconstructed, simulated, and measured idler spectrum with reconstructed spectral phase. (c) Typical soft X-ray probe spectrum generated with neon, extending in the water-window region, detected by the spectrometer camera (blue) and absorption spectrum of gas-phase dimethyl disulfide (DMDS, green). The sulfur L edges and carbon K edge are simultaneously resolved, and the energy of other atomic edges is labeled.

as in [7,8,22] with similar setups and infrared driving pulses. We can thus confidently assume a sub-femtosecond duration for the isolated probe pulse.

The pump pulses are generated via a two-stage HCF system using the signal pulses. The signal pulses from the OPA (1.45  $\mu m$ ) enter a stretched HCF filled with an increasing gradient pressure of argon. The pulses are then compressed to 10 fs [2.1 optical cycles, Fig. 3(a)] with reflections off a chirped mirror complementary pair. The pulses pass through an attenuator consisting of an achromatic half-wave plate and a silicon plate at Brewster's angle and are then focused into a second HCF.

The pump pulses are generated in the second HCF via an RDW process. In traditional HCF spectral broadening, non-linear processes, most notably self-phase modulation, dominate and dispersion is only provided post-broadening by chirped mirrors and/or bulk compressors. However, when a shorter pulse is guided through a sufficiently long gas-filled HCF, the higher intensity and larger dispersion induced by the waveguide causes dispersive effects within the fiber, and when both processes are balanced, the pulse experiences soliton self-compression. Upon extreme

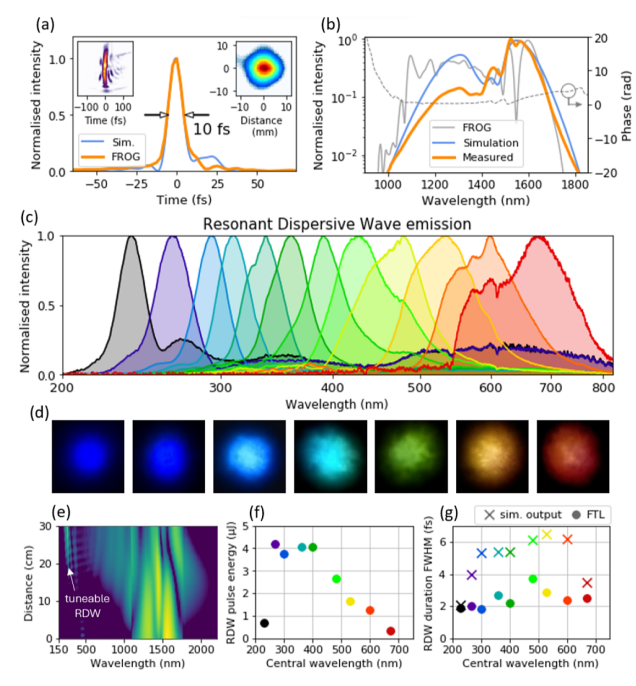


**Fig. 3.** (a) Temporal profile of the few-cycle signal pulses used to drive the RDW process. Left inset: SHG-FROG trace. Right inset: signal beam profile. (b) Reconstructed, simulated, and measured signal spectrum with reconstructed spectral phase. (c) Normalized measured spectra showing the continuous tuneability of the RDW emission from 230 to 700 nm (0.8–7.2 bars of argon). (d) Color photographs of the RDW far-field mode on white paper at different gas pressures; UV beams are visible due to the fluorescence of white paper, the latter appearing black here. (e) Simulated pulse propagation in the HCF, with the RDW emission labelled. (f) Measured RDW pulse energy at different central wavelengths. (g) Simulated RDW pulse duration at the fiber output at different central wavelengths with Fourier-transform-limited (FTL) duration.

self-compression, soliton fission occurs and an RDW is emitted in the UV-Vis region [17].

We used the Luna.jl code [23] to simulate the pulse propagation in the HCF and design our setup. Following these simulations, we built a 30-cm-long RDW stretched hollow capillary fiber with an inner diameter of 180 µm filled with argon. Dispersion in argon is higher compared to neon or helium allowing us to work at a lower gas pressure, thus reducing drastically the vacuum pumping requirement at the fiber exit. The counterpart is the lower ionization potential of argon, which limits the input intensity due to a plasma formation and thus clamps the RDW conversion efficiency [24]. Contrary to the first fiber, where the entrance cell is evacuated to prevent plasma formation, here the gas is injected into the entrance cell and the exit is directly in vacuum in order to produce shorter pulses [25]. This setup is able to produce widely tuneable RDW pulses, with several microjoules of energy, reaching the gigawatt peak power level (Fig. 3). The accessible RDW tuneability range (230-700 nm) is dictated by the wavelength of the driver (1.45 µm) [17]. The experimental results are in good agreement with our simulations; see Supplement 1. The continuous tunability of the RDW pulses is easily achieved by modifying the gas pressure with a regulator and the input energy with the attenuator.

The pulses exiting the fiber in vacuum are then transported to the target. The beam is collimated using a spherical UV-enhanced aluminium (UV-Al) mirror (Layertec 124315) and is reflected off

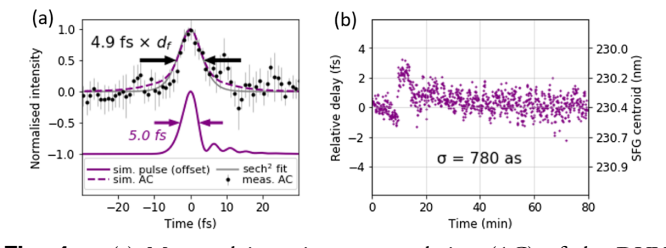


**Fig. 4.** (a) Measured intensity autocorrelation (AC) of the DUV pump pulse after propagation (with errorbars and sech<sup>2</sup> fit) and simulated AC from the simulated pulse temporal profile (offset). Deconvolution factor:  $d_f = 1.545$ . (b) Attosecond interferometric stability of the setup measured on the target with type II SFG between the chirped DUV and the idler pulses.

four high-reflectivity (HR) broadband mirrors with low groupdelay dispersion (GDD) (Edmund Optics 11-735), to avoid any large temporal distortion of the ultrashort pulses. The purpose of these mirrors is to separate the RDW pulse from the infrared driving field (~10% reflectivity per mirror in the infrared). We choose to operate at 270 nm as very few broadband HR low-GDD dichroic mirrors are yet commercially available. Thus the tuneability of the RDW pulses on the target requires a change of the beamline mirrors. The optics to separate the RDW from the driving field is the bottleneck of this technique [26]. We plan to overcome this issue with custom ultra-broadband mirrors. The use of silicon plates at Brewster's angle is another technique to separate the RDW emission but is only viable in the deep-UV (DUV) range and the losses are very high (>75%) [27]. After removing the unconverted infrared component, the DUV pulses go through an ultrathin CaF<sub>2</sub> plate to compensate for the small negative GDD accumulated during the pulse propagation. The pump beam is then focused in vacuum and recombined with the probe using a D-shaped mirror in a quasi-collinear 2f-2f configuration using the toroidal mirror to reimage the pump focal spot on the target.

While these few-fs RDW pulses are now well characterized at the fiber output [27,28], keeping their ultrashort duration and energy during transport on the target remains challenging [24,26]. Here, we measured the pump pulse duration on the target, in vacuum, with an all-reflective intensity autocorrelator [29] using a wavelength-independent and dispersion-free photosensitive asymmetric nanogap detector with a non-linearity close to two [30]. The Al/Au nanogaps were fabricated by adhesion-lithography [31] (see Supplement 1). Matching the simulations including pulse propagation, Fig. 4(a) presents the 4.9-fs full width at half maximum (FWHM) pump pulse duration measured on the target. By using custom ultra-low GDD dichroic mirrors, we plan to achieve sub-4-fs pump pulses on the target (see Supplement 1). In our few-fs pump/attosecond probe setup, the time-resolution of the system is defined by the pump pulse duration, here sub-5 fs at 270 nm. The duration of pump pulses produced at higher wavelengths should remain below 7 fs on the target with standard dichroic mirrors (see Supplement 1) and can be shortened with custom optics.

With a measured energy of 1.9  $\mu$ J, a focal spot diameter of 104  $\mu$ m at 1/e<sup>2</sup> and an FWHM pulse duration of 4.9 fs, the pump peak intensity, on the target at 270 nm central wavelength, can reach up to 8 TW/cm<sup>2</sup> (peak fluence: 45 mJ/cm<sup>2</sup>).

The interferometric stability of an ultrafast pump/probe setup is crucial to ensure a few-femtosecond resolution over a time-resolved experimental scan that can take a few hours. The

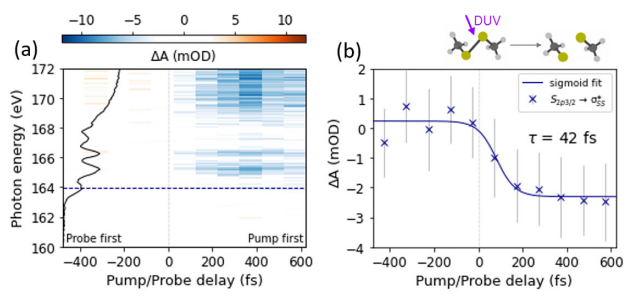


**Fig. 5.** (a) TR-XAS map, at the sulfur L<sub>2,3</sub> edge, following the photodissociation of DMDS initiated by a DUV pump pulse. This coarse scan shows the ability of the RDW pump to initiate a photochemical reaction. Black line: DMDS absorption spectrum. (b) Lineout of the  $S_{2p^3/2} \rightarrow \sigma_{SS}^*$  feature [dashed dark blue line in (a)]. A decay time of 42 fs is observed.

interferometric stability of our system has been measured with a non-linear interaction between the DUV pump pulses and the idler pulses [Fig. 4(b)]. We used type II SFG in a thin beta barium borate crystal placed at the interaction point. The generated signal at ~230 nm allows us to find the temporal overlap between the two pulses. Moreover, by inducing some chirp in the DUV beam, we are able to find a relation between the centroid wavelength of the SFG signal and the relative delay between the pulses (see Supplement 1). By recording the centroid wavelength of the SFG signal, we are able to extract the interferometric stability of our setup. We measured a sub-femtosecond stability (standard deviation: 0.780 fs) over 80 min without any active interferometric stabilization, during a standard workday. This is confirmed by the fact that our stage position for which we have a temporal overlap is usually unchanged from day to day.

The target chamber can hold different types of samples: solid films [4], ultrathin liquid jets [32,33], or vapor phase samples. For our first experiment using RDW pump pulses, we chose to use dimethyl disulfide (DMDS) in vapor phase to test our setup with an experiment previously presented in [3]. Since UV excitation induces photodissociation in DMDS, a long-lived step-like decrease in absorption is observed in the sulfur L<sub>2,3</sub> pre-edge features due to the breaking of the S-S bond. The well-defined ultrafast signal allowed us to confirm the pump/probe overlap. Crucially, this confirms that RDW pulses are capable of initiating photochemical dynamics and have sufficient intensity to pump an observable absorption change ( $\Delta A$ ) for TR-XAS experiments. The results are shown in Fig. 5 and agree with reported values [3]. Future studies will present much finer scans resolving faster electronic dynamics at different atomic edges. See Supplement 1 for additional results at the carbon K edge.

These new capacities for TR-XAS will allow studies of the fastest electronic motions in a large range of small molecules and photoactive polymers [34]. The creation of superpositions of valence electronic states with the broadband few-fs pump pulses promises control over photochemical reactions, opening the way to attochemistry studies [35].

**Funding.** Engineering and Physical Sciences Research Council (EP/T020903/1, EP/V026690/1); UK Research and Innovation (MR/V024442/1); Royal Academy of Engineering (RF/202122/21/133); H2020 European Research Council (101001534).

**Acknowledgment.** We thank S. Parker and A. Gregory for technical work and D. Garratt and T. Barnard for early work. JCT is supported by a Chair in Emerging Technology from the Royal Academy of Engineering and by the Institution of Engineering and Technology.

**Disclosures.** The authors declare no conflicts of interest.

**Data availability.** Data underlying the results presented in this paper are not publicly available at this time but may be obtained from the authors upon reasonable request.

**Supplemental document.** See Supplement 1 for supporting content.

## **REFERENCES**

- I. C. Merritt, D. Jacquemin, and M. Vacher, J. Phys. Chem. Lett. 12, 8404 (2021).
- 2. P. M. Kraus, M. Zürch, S. K. Cushing, et al., Nat. Rev. Chem. 2, 82 (2018).
- K. Schnorr, A. Bhattacherjee, K. J. Oosterbaan, et al., J. Phys. Chem. Lett. 10. 1382 (2019).
- 4. D. Garratt, L. Misiekis, D. Wood, et al., Nat. Commun. 13, 3414 (2022).
- 5. Z. Yin, Y.-P. Chang, T. Balčiūnas, et al., Nature 619, 749 (2023).
- A. M. Summers, S. Severino, M. Reduzzi, et al., Ultrafast Sci. 3, 0004 (2023).
- 7. T. Gaumnitz, A. Jain, Y. Pertot, et al., Opt. Express 25, 27506 (2017).
- 8. F. Silva, S. M. Teichmann, S. L. Cousin, et al., Nat. Commun. 6, 6611 (2015).
- K. S. Zinchenko, F. Ardana-Lamas, I. Seidu, et al., Science 371, 489 (2021).
- 10. R. B. Varillas, A. Candeo, D. Viola, et al., Opt. Lett. 39, 3849 (2014).
- L. Bruder, L. Wittenbecher, P. V. Kolesnichenko, et al., Opt. Express 29, 25593 (2021).
- 12. R. Piccoli, J. Brown, Y.-G. Jeong, et al., Nat. Photonics 15, 884 (2021).
- 13. Y. Jiang, J. P. Messerschmidt, F. Scheiba, et al., Optica 11, 291 (2024).
- 14. L. Barreau, A. D. Ross, S. Garg, et al., Sci. Rep. 10, 5773 (2020).
- K. S. Zinchenko, F. Ardana-Lamas, V. U. Lanfaloni, et al., Sci. Rep. 13, 3059 (2023).
- 16. Z. Guo, T. Driver, S. Beauvarlet, et al., Nat. Photonics 18, 691 (2024).
- J. C. Travers, T. F. Grigorova, C. Brahms, et al., Nat. Photonics 13, 547 (2019).
- 18. C. Brahms, F. Belli, and J. C. Travers, Phys. Rev. Res. 2, 043037 (2020).
- D. R. Austin, T. Witting, S. J. Weber, et al., Opt. Express 24, 24786 (2016).
- A. S. Johnson, L. Miseikis, D. A. Wood, et al., Struct. Dyn. 3, 062603 (2016).
- A. S. Johnson, D. R. Austin, D. A. Wood, et al., Sci. Adv. 4, eaar3761 (2018).
- 22. J. Li, X. Ren, Y. Yin, et al., Nat. Commun. 8, 186 (2017).
- C. Brahms and J. Travers, "Luna. jl: a flexible nonlinear optical pulse propagator," (2021).
- 24. N. Kotsina, C. Brahms, S. L. Jackson, et al., Chem. Sci. 13, 9586 (2022).
- 25. C. Brahms, F. Belli, and J. C. Travers, Opt. Lett. 45, 4456 (2020).
- 26. C. Brahms and J. C. Travers, APL Photonics 9, 050901 (2024).
- 27. M. Reduzzi, M. Pini, L. Mai, et al., Opt. Express 31, 26854 (2023).
- 28. C. Zhang, T. Chen, J. Pan, et al., Opt. Lett. 47, 4830 (2022)
- 29. A. Tyagi, M. S. Sidhu, A. Mandal, et al., Sci. Rep. 12, 8525 (2022).
- H. Ning, M. Maimaris, J. Wei, et al., "Ultrafast broadband strong-field tunnelling in asymmetric nanogaps for time-resolved nanoscopy," arXiv (2024).
- D. G. Georgiadou, J. Semple, A. A. Sagade, et al., Nat. Electron. 3, 718 (2020).
- J. C. Barnard, J. P. Lee, O. Alexander, et al., Front. Mol. Biosci. 9, 1044610 (2022).
- 33. C. Ferchaud, S. Jarosch, T. Avni, et al., Opt. Express 30, 34684 (2022).
- 34. D. Garratt, M. Matthews, and J. Marangos, Struct. Dyn. 11, 010901
- 35. F. Calegari and F. Martin, Commun. Chem. 6, 184 (2023).